Journal of Turkish

Operations Management

Optimization of nanofiber diameter in the electrospinning of polyamide 6 by two-level factorial design

Deniz Efendioğlu[1*], Serife Akkoyun[2,3]

[1]Department of Industrial Engineering, Faculty of Engineering and Natural Sciences, Ankara Yildirim Beyazit University, 06010 Ankara, Türkiye
e-mail: defendioglu@aybu.edu.tr, ORCID: https://orcid.org/0000-0002-3710-9187
[2]Department of Metallurgical and Materials Engineering, Faculty of Engineering and Natural Sciences, Ankara Yildirim Beyazit University, 06010 Ankara, Türkiye
[3]Central Research Laboratory, Application and Research Center, Ankara Yildirim Beyazit University, 06010 Ankara, Türkiye
e-mail: serife.akkoyun@aybu.edu.tr, ORCID: https://orcid.org/0000-0002-6676-6389
*Corresponding Author

Article Info

Article History:
Received: 19.09.2023
Revised: 09.12.2023
Accepted: 29.01.2024

Keywords
Factorial Design,
Polyamide 6,
Optimization,
Nanofibers,
Electrospinning

Abstract

The utilization of 2-level factorial design has been extensive in the literature to observe the relationship between parameters and responses. Among the subjects open for exploration, the process of nanofiber creation stands out as an intriguing avenue to explore the correlations that emerge between variables and outcomes. The primary objective of the study is to establish the relationship between the parameters of electrospinning of polyamide 6 (PA6) solutions to obtain desired nanofiber diameters by two level full factorial design. The investigation hones in on four critical parameters related to the electrospinning process of PA6 solutions. These parameters are solution concentration, applied voltage, distance between the spinneret and the collector, and the flow rate of the solution. Employing a two-level factorial design, these parameters are methodically manipulated at two distinct levels each to systematically unravel their individual and collective impacts on nanofiber diameter outcomes. After the model is obtained, the full model was fitted to first response. In the step of identifying important variables, background elimination and forward selection was chosen. Clearly polymer concentration have strong effect on the response and the effects of other main factors and interactions are explained in detail.

1. Introduction

The control of the electrospinning process ensures that the products are obtained as desired. From this point of view, it is aimed to make clear studies on fiber size and morphology by looking at various levels of parameters related to the electrospinning process and developing models. The fiber diameter achieved in electrospinning determines various properties of the electrospun fiber mats, including mechanical, electrical, and optical properties.

The process of determining which effects should be chosen for significant impact has been investigated in numerous studies. Thompson et. al. (2007) stated this by examining the effects of 13 materials and operating parameters on electrospun fiber diameters. The study of Naderi et al. (2008) has similarities with the previous study except that they used a response function and central composite design (CCD). He et al. (2020) conducted an examination of the impact of alternating current (AC) on the diameter and orientation of electrospun nanofibers using the Box-Behnken Methodology. In a related study, Filip et al. (2019) proposed a mathematical model to clarify the relationship between the mean diameter and solution parameters in the electrospinning of poly(ethylene oxide) nanofibers.

Various methods have been employed by different authors to investigate nanofiber diameter, such as Sukigara et al. (2004), who explored the spinning of regenerated nanoscale silk fibers from domestic silkworms. Additionally, the experimental method of response surface methodology (RSM) has been applied to model and optimize electrospinning parameters. In recent times, Fatile et al. (2021) have pursued a similar objective by aiming to

comprehend the impact of process parameters on niobium–tungsten oxide nanofibers and optimizing the process using a central composite design (CCD). Furthermore, Zeraati et al. (2021) delved into the study of Nylon-6,6 nanofibers for protection against coronavirus and employed gene expression programming (GEP) and genetic algorithms (GA) in their research.

Other methodologies were also proposed for solving the issue. Ketabchi et. al. (2017) studied an artificial neural network (ANN) model. Nasouri et. al. (2012) compared the ANN and experimental design of the Box-Behnken Method for the estimation of electrospun polyacrylonitrile (PAN) nanofiber diameter. Kalantari et al. (2020) proposed an approach that combines a multiple linear regression (MLR) model with an ANN model. According to the authors, MLR did not yield better results than ANN. In a similar vein, Kalantari et al. (2019) compared the performance of the multi-layer perception (MLP), radial basis function (RBF), and support vector machine (SVM) models for development of mathematical models to predict the diameter of poly(ε-caprolactone) (PCL)/gelatin (Gt) nanofibers. Likewise, Khalili et al. (2016) investigated the utility of RSM and artificial neural networks (ANNs).

The purpose of the optimizations can be separated in different topics. Zeraati et. al. (2021) studied Nylon-6,6 nanofibers for protection against coronavirus. Acatay et al. (2004) investigated the resultant hydrophobic behavior for PAN fibers. Ahmadipourroudposht et. al. (2015) researched the process of fabrication of magnetic nanofibers using polyvinyl alcohol (PVA) as a shelter for (γ-Fe2O3) nanoparticles. Amiri et. al. (2018) examined the fabrication of chitosan-collagen nanofibers to find optimum diameter.

The aim of this study is to find the relations between the parameters of electrospinning process of PA6 solutions on the nanofiber diameters by RSM and two level full factorial design. The effects of feed rate, tip-to-collector distance, voltage, and polymer concentration were studied within the context of two-level factorial design and RSM.

2. Materials & Methods

2.1. Materials

Polyamide 6 pellets were purchased from EUROTEC (Tecomid NB40 NL E, unfilled, natural), while formic acid with a purity range of 89–91% was obtained from Merck and used as a solvent for preparing the polymer solutions.

2.2. Design of Experiments

Minitab Statistical Software Version 21.4.1 was used to create a full-factorial design of experiments within a constrained region to establish a significant relationship between electrospinning parameters and polymer nanofiber diameter. Feed rate, spinning distance (tip-to-collector), voltage and polymer concentration are the four variables which were used for modeling.

The parameters are differentiated into four factors:

- Factor A: Feed rate (2–4 ml/h),
- Factor B: Tip-to-collector distance “Spinning distance” (5–8 cm),
- Factor C: Voltage (6–10 kV),
- Factor D: Polymer concentration (10–20%, w/w).

Randomized experiments were constructed for a 2-level factorial design. The standard runs for the experiments were determined, and then they were randomly chosen not to face experimental and observational errors. The responses to diameters were obtained, and investigated for this study. The constrained region were identified by the conditions of the experiments. The design contains 16 experiments as shown in Table 1.

2.3. Electrospinning

The electrospinning of polyamide 6 (PA6) nanofibers was performed as described by Akkoyun et al. (2021). In the first step, PA6 pellets were dissolved in formic acid to prepare the electrospinning solutions of different concentrations, provided in Table 1, under constant stirring at room temperature.

Then, PA6 nanofibers were electrospun with an electrospinning device (GAYDA Enerji, Türkiye) and using the processing parameters are gathered in Table 1.

2.4. Characterization of the nanofibers

The morphology and diameter of the nanofibers were assessed using a HITACHI SU5000 scanning electron microscope at 15 kV. All the samples were sputter coated with gold (Au) before observation. The average fiber diameter was measured with the SEM micrographs using ImageJ software (NIH-USA) from 100 fibers/samples.

Table 1. Process parameters obtained from the full factorial experimental design

		Factor A	Factor B	Factor C	Factor D
Std	Run	Feed Rate (mL)	Tip-to-Collector Distance (cm)	Voltage (kV)	Polymer Concentration (wt.%)
1	1	0.325	12.5	13.75	12.5
7	2	0.325	17.5	21.25	12.5
14	3	0.775	12.5	21.25	17.5
5	4	0.325	12.5	21.25	12.5
12	5	0.775	17.5	13.75	17.5
3	6	0.325	17.5	13.75	12.5
11	7	0.325	17.5	13.75	17.5
10	8	0.775	12.5	13.75	17.5
15	9	0.325	17.5	21.25	17.5
9	10	0.325	12.5	13.75	17.5
6	11	0.775	12.5	21.25	12.5
8	12	0.775	17.5	21.25	12.5
16	13	0.775	17.5	21.25	17.5
4	14	0.775	17.5	13.75	12.5
13	15	0.325	12.5	21.25	17.5
2	16	0.775	12.5	13.75	12.5

2.5. Explanation of the Process

In the process of calculating significant ranges for input variables have to be determined carefully. It should be large enough to contain the possible parameter space and not to increase the difference of the response surface to actual response. Fiber sample obtained from each experiment run were taken using electron microscopy and studied by observing their fiber morphology and spinning behaviour.

3. Results & Discussion

3.1. Properties of the nanofibers

The SEM micrographs of the nanofibers obtained from the different runs listed in Table 1 are given in Figure 1.

The 16 experimental conditions allowed to produce nanofibers with various morphologies as cylindrical, beaded or with extra webs. As shown in Figure 1, continuous cylindrical nanofibers with a homogeneous diameter were obtained in case f) (run 12). In cases b) (run 2) and g) (run 14), cylindrical nanofibers with different diameters were observed. Although nanofibers were obtained in the other runs, only a few nanofibers are present in case a) (run 1) and the others present nanofibers with different diameters but the presence of thinner extra webs is also noticeable.

The diameters of the nanofiber were also determined from the SEM images. The average diameters corresponding to each sample are given in Table 2. For the statistical analyses, the diameter is qualified as Response 1 and was used to describe the relationships between the different parameters. The average diameters of the nanofibers vary from 90 nm to 205 nm. The best compromise between the morphology and the diameter of the nanofibers was obtained for run 12 where the polymer concentration is 12.5 wt.%.

3.2. Two-Level Factorial Experimental Design

A preliminary screening study was conducted to determine the main factors and their interactions on the response of the study.

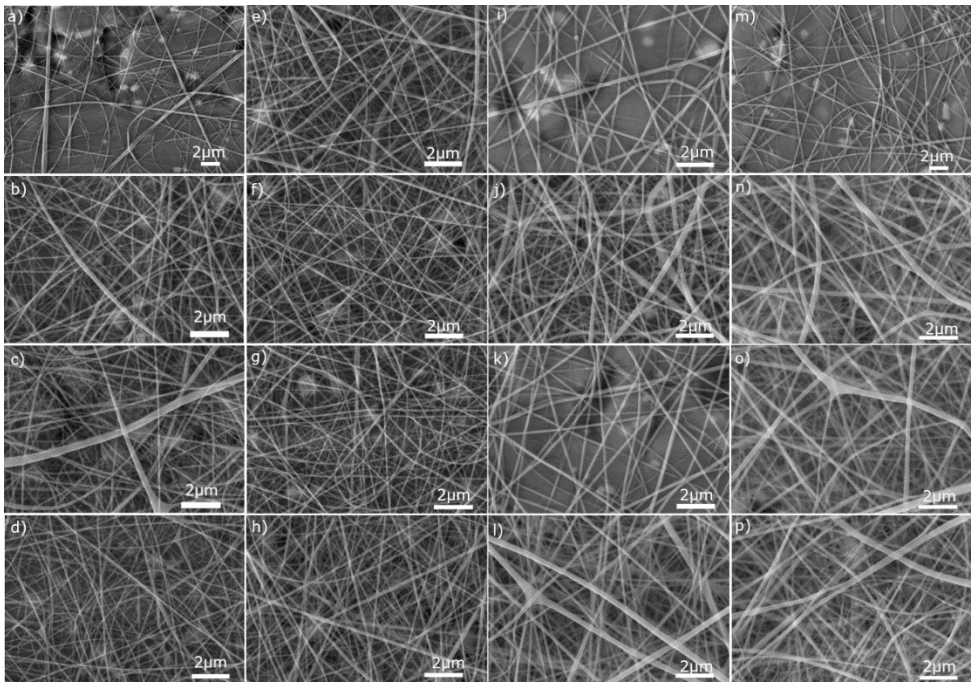

Figure 1. SEM micrographs of the nanofibers produced from a) run 1, b) run 2, c) run 4, d) run 6, e) run 11, f) run 12, g) run 14, h) run 16, a) run 3, j) run 5, k) run 7, l) run 8, m) run 9, n) run 10, o) run 13 and p) run 15

Table 2. Experimental results obtained from the different process parameters designed. The diameter is qualified as Response 1 was used to describe the relationships between the different parameters.

		Factor A	Factor B	Factor C	Factor D	Response 1
Std	Run	Feed Rate (mL)	Tip-to-Collector Distance (cm)	Voltage (kV)	Polymer Concentration (wt.%)	Diameter (nm)
1	1	0.325	12.5	13.75	12.5	.120
7	2	0.325	17.5	21.25	12.5	107
14	3	0.775	12.5	21.25	17.5	145
5	4	0.325	12.5	21.25	12.5	125
12	5	0.775	17.5	13.75	17.5	147
3	6	0.325	17.5	13.75	12.5	90.0
11	7	0.325	17.5	13.75	17.5	126
10	8	0.775	12.5	13.75	17.5	149
15	9	0.325	17.5	21.25	17.5	173
9	10	0.325	12.5	13.75	17.5	159
6	11	0.775	12.5	21.25	12.5	118
8	12	0.775	17.5	21.25	12.5	97.0
16	13	0.775	17.5	21.25	17.5	171
4	14	0.775	17.5	13.75	12.5	93.0
13	15	0.325	12.5	21.25	17.5	205
2	16	0.775	12.5	13.75	12.5	108

The feed rate (Factor A), the tip-to-collector distance (Factor B), the high voltage applied (Factor C) and the concentration of the polymer (Factor D) were considered as factors for this purpose. Blocking and confounding were not required and completely randomized design is found enough to go on in this experiment. The full model was fitted to the first response. In this step we would have liked to compare the results of forward selection and

backward elimination to identify important variables. They were classified respectively as first model and second model for the experiment. In forward selection, main factors and interactions were entered into the equation one by one and at the last step the main factors B, C, D were selected. The results can be seen in Table-3. α was taken as 0.1. Then, backward elimination was used to determine the equation. Firstly, all interactions and main factors are included, secondly the insignificant parameters are excluded from the equation.

Table 3. Forward Selection of Terms (Candidate terms: A; B; C; D; A*B; A*C; A*D; B*C; B*D; C*D; A*B*C; A*B*D; A*C*D; B*C*D; A*B*C*D)

	-----Step 1----		**-----Step 2----**		**-----Step 3----**	
	Coef	**P**	**Coef**	**P**	**Coef**	**P**
Constant	133.31		133.31		133.31	
D	26.06	0.000	26.06	0.000	26.06	0.000
C			9.31	0.048	9.31	0.032
B					-7.81	0.064
S		19.2416		17.0876		15.3277
R-sq		67.71%		76.35%		82.44%
R-sq(adj)		65.40%		72.71%		78.05%
R-sq(pred)		57.82%		64.18%		68.78%
AICc		145.90		144.55		144.15
BIC		146.21		144.00		142.02

α to enter = 0,1

At last, A, B, C, D main factors and AB interactions are selected for the last result. The equation can be seen in Table-4 and 9. In the process of selecting variables for inclusion in the model, the hierarchy principle are followed and all main effects are kept that are part of significant higher-order terms or interactions, even if the main effect p-value is larger than expected.

Table 4. Backward Elimination of Terms **(**Candidate terms: A; B; C; D; A*B; A*C; A*D; B*C; B*D; C*D; A*B*C; A*B*D; A*C*D; B*C*D; A*B*C*D)

	-----Step 1----		**-----Step 2----**		**-----Step 3----**		**-----Step 4----**	
	Coef	**P**	**Coef**	**P**	**Coef**	**P**	**Coef**	**P**
Constant	133.31		133.31		133.31		133.31	
A	-4.81	0.068	-4.81	0.114	-4.81	0.162	-4.81	0,136
B	-7.81	0.016	-7.81	0.027	-7.81	0.041	-7.81	0,029
C	9.31	0.009	9.31	0.014	9.31	0.022	9.31	0,014
D	26.06	0.000	26.06	0.000	26.06	0.000	26.06	0,000
A*B	6.31	0.031	6.31	0.054	6.31	0.082	6.31	0,063
A*C	-5.06	0.060	-5.06	0.100	-5.06	0.145	-5.06	0,120
A*D	-1.56	0.466	-1.56	0.561	-1.56	0.623		
B*D	2.69	0.239	2.69	0.334	2.69	0.408	2.69	0,378
C*D	4.81	0.068	4.81	0.114	4.81	0.162	4.81	0,136
A*B*D	4.81	0.068	4.81	0.114				
A*C*D	-4.06	0.105						
S		7.76611		10.0530		12.0822		11,4326
R-sq		98.50%		96.85%		94.54%		94,30%
R-sq(adj)		94.36%		90.56%		86.36%		87,79%
R-sq(pred)		75.95%		67.76%		61.20%		70,22%
AICc		296.82		228.65		197.45		174,15
BIC		124.86		133.92		139.95		137,87

	-----Step 5----		-----Step 6----		-----Step 7----	
	Coef	**P**	**Coef**	**P**	**Coef**	**P**
Constant	133.31		133.31		133.31	
A	-4.81	0.128	-4.81	0.157	-4.81	0.183
B	-7.81	0.025	-7.81	0.034	-7.81	0.043
C	9.31	0.011	9.31	0.015	9.31	0.020
D	26.06	0.000	26.06	0.000	26.06	0.000
A*B	6.31	0.057	6.31	0.074	6.31	0.090
A*C	-5.06	0.112	-5.06	0.139		
A*D						
B*D						
C*D	4.81	0.128				
A*B*D						
A*C*D						
S		11.3496		12.4769		13.4578
R-sq		93.58%		91.27%		88.72%
R-sq(adj)		87.96%		85.45%		83.08%
R-sq(pred)		74.32%		72.41%		71.11%
AICc		160.05		153.54		149.07
BIC		137.00		139.15		140.48

α to remove = 0,1

*The initial model was saturated. The stepwise procedure removed the following terms in order to obtain sufficient degrees of freedom to begin: B*C; A*B*C; B*C*D; A*B*C*D*

These two results were selected for the reason that the first model has the lowest value of AICc, value with 3 significant factors for α=0.1 (almost can be said for α=0.05) and the second one have the highest R sq, Adj R sq and Pred. R sq and not possessing too much high value of BIC value from Table-9. Furthermore, at the first model p value of the coefficients are lower than 0.1 and also 0.05; except for the factor B, which is lower than 0.1, but higher than 0.05. At the second model, p value of the coefficients which are stated at the first model, still significant but AB interaction is between 0.05 and 0.10 and also factor A and AB interaction do not effect the result too much when we compare others.

When all models have been investigated through Table 5-6, it is clearly seen that the main factor coefficients have a clear effect on results. Therefore, the effect of linear coefficients must be investigated carefully. The polymer concentration exhibits a pronounced impact on the results when compared to the other parameters.

Table 5. Analysis of Variance of the first model

Source	**DF**	**Seq SS**	**Contribution**	**Adj SS**	**Adj MS**	**F-Value**	**P-Value**
Model	3	13232.2	82.44%	13232.2	4410.7	18.77	0.000
Linear	3	13232.2	82.44%	13232.2	4410.7	18.77	0.000
B	1	976.6	6.08%	976.6	976.6	4.16	0.064
C	1	1387.6	8.64%	1387.6	1387.6	5.91	0.032
D	1	10868.1	67.71%	10868.1	10868.1	46.26	0.000
Error	12	2819.3	17.56%	2819.3	234.9		
Total	15	16051.4	100.00%				

Table 6. Analysis of Variance of the second model

Source	DF	Seq SS	Contribution	Adj SS	Adj MS	F-Value	P-Value
Model	5	14240.3	88.72%	14240.3	2848.1	15.73	0.000
Linear	4	13602.8	84.74%	13602.7	3400.7	18.78	0.000
A	1	370.6	2.31%	370.6	370.6	2.05	0.183
B	1	976.6	6.08%	976.6	976.6	5.39	0.043
C	1	1387.6	8.64%	1387.6	1387.6	7.66	0.020
D	1	10868.1	67.71%	10868.1	10868.1	60.01	0.000
2-Way Interactions	1	637.6	3.97%	637.6	637.6	3.52	0.090
A*B	1	637.6	3.97%	637.6	637.6	3.52	0.090
Error	10	1811.1	11.28%	1811.1	181.1		
Total	15	16051.4	100.00%				

3.3. Regression analysis

Coded and uncoded coefficients of equations were also examined and the results are gathered in Table-7. It is absolutely observed that the coefficient of factor D (polymer concentration) is the highest one in every equation and the significance of this factor can be seen in determining the main effects. The coefficients of B, C and D variables are found significant in regression equation for the first model. Then, except from B, C and D are still found significant. The factor B is also remarkably close to the value of 0.05. Therefore, they can be put into the equation to see their specific result on the equation. The coefficients of A, B, C and D main factors and AB interaction are found significant in the regression equation for the second model. Besides, except from AB and A, C and D are also found significant. It can be observed that, factor A is not too close to the value of significant value, but due to the hierarchy principle and effect of AB interaction, it was put to the equation.

Table 7. Coded Coefficients of the first model

Term	Effect	Coef	SE Coef	95% CI	T-Value	P-Value	VIF
Constant		133.31	3.83	(124.96; 141.66)	34.79	0.000	
B	-15.63	-7.81	3.83	(-16.16; 0.54)	-2.04	0.064	1.00
C	18.63	9.31	3.83	(0.96; 17.66)	2.43	0.032	1.00
D	52.13	26.06	3.83	(17.71; 34.41)	6.80	0.000	1.00

Table 8. Coded Coefficients of the second model

Term	Effect	Coef	SE Coef	T-Value	P-Value	VIF
Constant		133.31	3.36	39.62	0.000	
A	-9.63	-4.81	3.36	-1.43	0.183	1.00
B	-15.63	-7.81	3.36	-2.32	0.043	1.00
C	18.63	9.31	3.36	2.77	0.020	1.00
D	52.12	26.06	3.36	7.75	0.000	1.00
A*B	12.63	6.31	3.36	1.88	0.090	1.00

3.4. Tests & Models

The statistical and regression analysis parameters are gathered in Figure-2 and Figure-3. It can be seen from Table-9 that high R^2 and adjusted R^2 values can be obtained. The second analysis provided better results for R^2 values.

However, the value of AICc is in second analysis higher than the first analysis one and non-significant parameters (factor A higher than α=0.1 and the interaction AB value almost equal) are added to the regression equation.

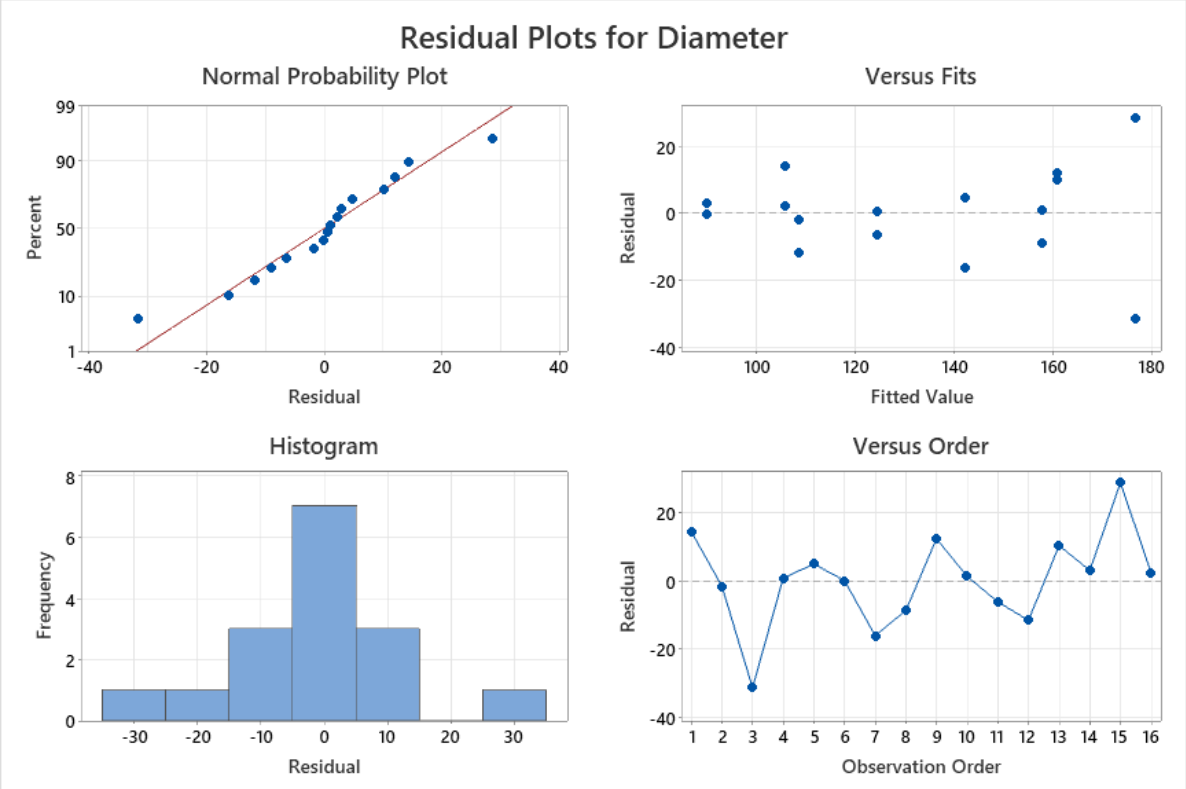

Figure 2. The residual plots of the first model

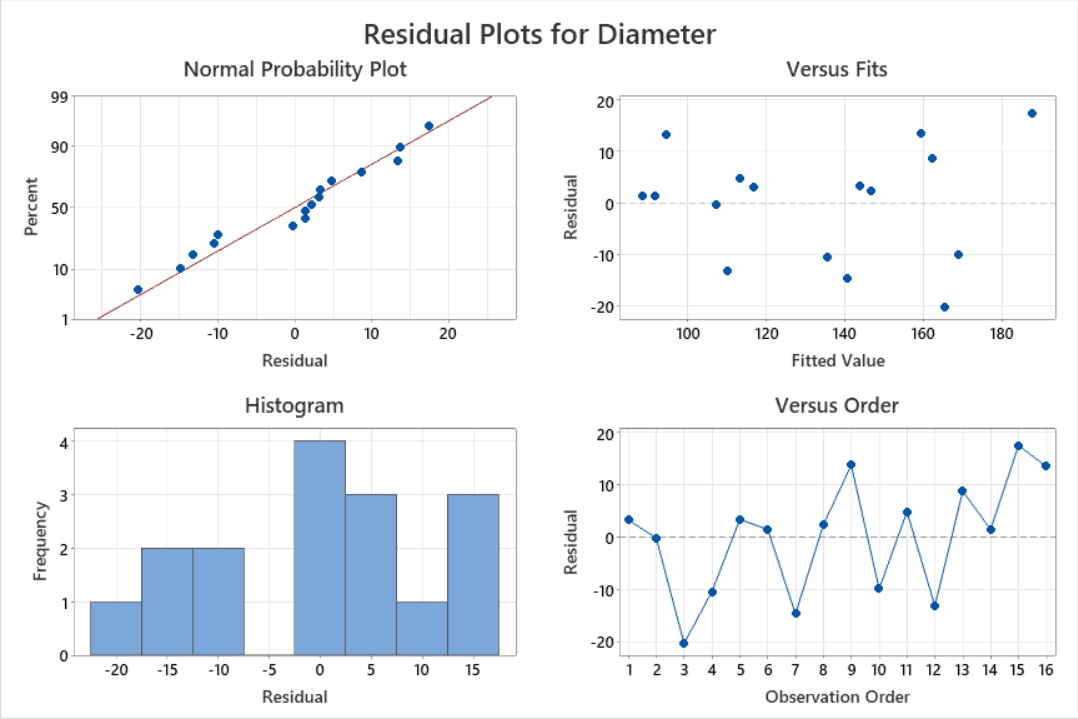

Figure 3. The residual plots of the second model

According to these results, the polymer concentration can directly have an effect on the fiber morphology. The surface tension has a decreasing trend on surface area and favors the formation of particles, while viscoelastic forces promote the formation of fibres (Amarieri et. al., 2017). The surface tension may have a high impact over viscoelastic forces at low polymer concentrations. On the other hand, a high viscosity makes the extension of the jet difficult and therefore thick fibres can be observed at high polymer concentrations.

Two level four factor design were included in this study and for different levels a second experimental design have been applied to understand the interactions between the parameters. To enhance the predictive capability of the model, it is essential to strike a balance between a well-defined operational range and sufficient inclusion of distant data points.

The distribution of first model maybe more fitted to normal distribution than the second one. The residuals were identically distributed. Independency are seen for both models and normal distribution can be observed for both models. The residual-observation order graph for the second model show a little oscillation. To sum up, all the information derived from residual analysis show that the suitability of first model is slightly better than the second model.

Table 9. Statistical results and uncoded coefficients of the models for 2 different alternatives

Model Summary-1			
S	**R-sq**	**R-sq (adj)**	**R-sq (pred)**
15.3277	82.44%	78.05%	68.78%
Model Summary-2			
S	**R-sq**	**R-sq(adj)**	**R-sq(pred)**
13.4578	88.72%	83.08%	71.11%

Regression Equation in Uncoded Units-1	
R1	-19.6 - 3.12 B + 2.48 C + 10.43 D
Regression Equation in Uncoded Units-2	
R1	84.7 - 189.7 A - 9.30 B + 2.483 C + 10.43 D + 11.22 A*B

Contour plots provided in Figures 4 and 5 show that for the first model, the effect of D compared to C and B is too much high. Also, for the second equation, the effect of D is still too high. Also the interaction of A and B can be observed from A-B contour plot.

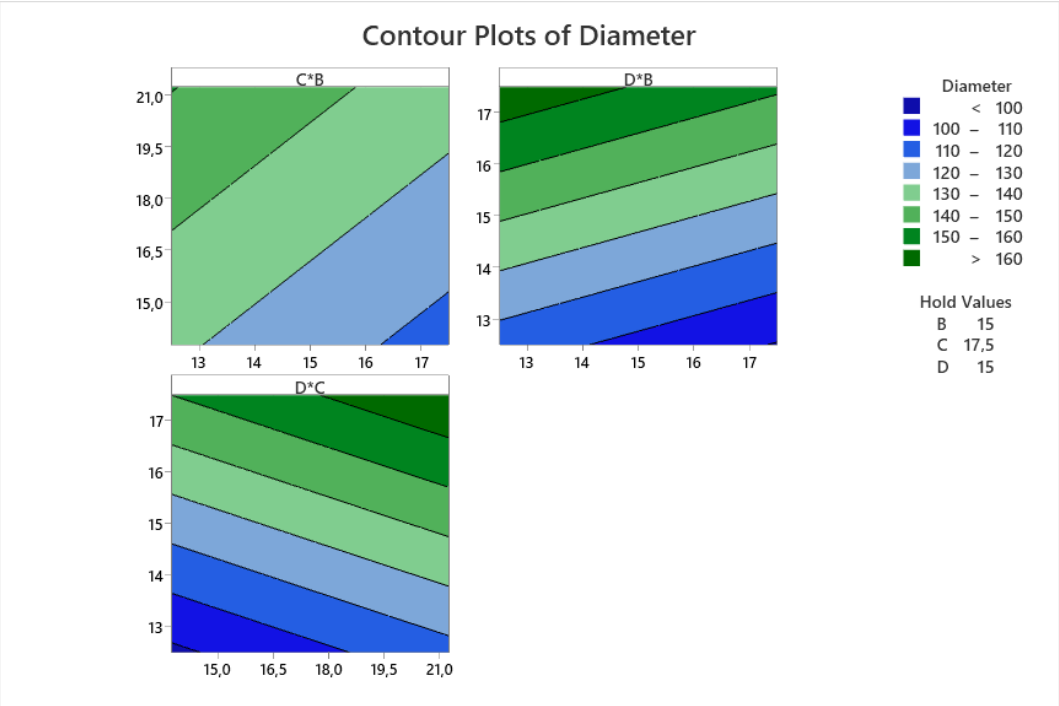

Figure 4. The contour plots of the first model

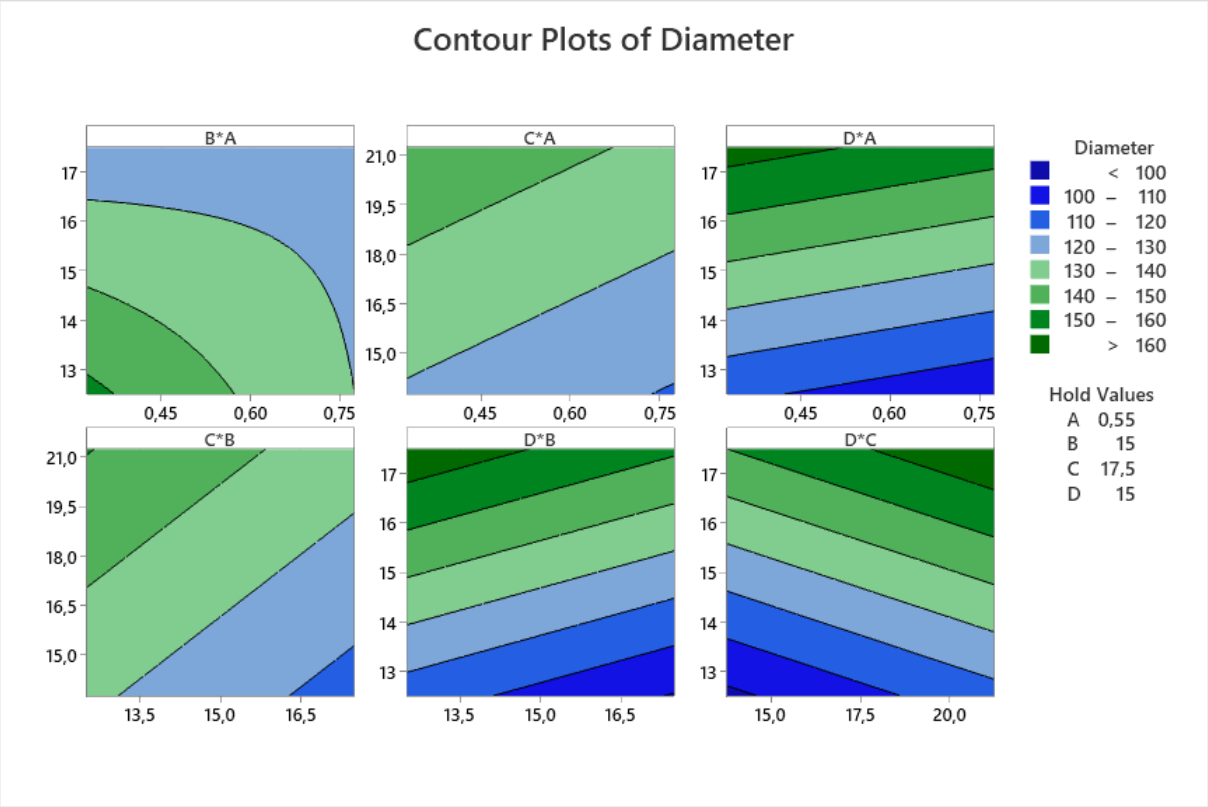

Figure 5. The contour plots of the second model

Taking the vectors of input and finding the relationship with outputs are the next step of the study at the end of computer runs and experiments. Developing an appropriate model depends on the true relationship between the inputs and outputs. The creation of experimental designs has been applied by using full factorial design. In this study, two-level-full factorial design was used in order to lower experimental combinations to procure maximum amount of information for a better evaluation of the model.

4. Conclusion

Two-level factorial design possesses a great capability of examining the affinity between the factor variables and outputs of experiments. Moreover, it also enables a thorough observation of the interactions between the variables. When the comparison of basic experimental/ optimization methods and one variable at a time technique are stated, this method has been useful for taking the results with much less data. For the first model, a two-level full factorial design revealed that the polymer concentration and the applied voltage directly influence the nanofiber diameter, whereas spinning distance exhibit an inverse relationship with the diameter of the produced nanofibers. For the second model, the same evolution is observed for the polymer concentration, applied voltage and spinning distance with the diameter of the produced nanofibers. The added parameters of feed rate, interaction of feed rate and spinning distance are also shown in the equation. The interaction has too much effect than feed rate. Their effects are not too much significant but they contribute to the explanation for understanding the equation of the second model. The main concluding remarks of this study are (1) The approach of the study provides new results compared to the literature. (2) The accurate design of the experiments can help researchers to find significant results with fewer experiment numbers. (3) These kinds of study is open to everyone in direction of future research on the electrospinning of different types of polymers.

Contribution of Authors

Deniz Efendioğlu carried out design and data analysis, methodology , experimental design, interpretation of model results, writing & editing. Şerife Akkoyun carried out conceptualization, investigation, resources, experimentation, data curation, methodology, writing-review & editing.

Conflict of Interest

The authors declared that there is no conflict of interest.

References

Acatay, K. (2004). Generation of superhydrophobic surfaces by electrospinning process (Doctoral dissertation) DOI: https://research.sabanciuniv.edu/id/eprint/8213

Ahmadipourroudposht, M., Fallahiarezoudar, E., Yusof, N. M., & Idris, A. (2015). Application of response surface methodology in optimization of electrospinning process to fabricate (ferrofluid/polyvinyl alcohol) magnetic nanofibers. Materials Science and Engineering: C, 50, 234-241. DOI: https://doi.org/10.1016/j.msec.2015.02.008

Akkoyun S., Öktem N., (2021), Effect of viscoelasticity in polymer nanofiber electrospinning: Simulation using FENE-CR model. Engineering Science and Technology, an International Journal, 24(3), 620-630 DOI: https://doi.org/10.1016/j.jestch.2020.12.017

Amariei, N., Manea, L. R., Bertea, A. P., Bertea, A., & Popa, A. (2017, June). The influence of polymer solution on the properties of electrospun 3D nanostructures. In IOP conference series: Materials science and engineering (Vol. 209, No. 1, p. 012092). IOP Publishing. DOI: https://doi.org/10.1088/1757-899X/209/1/012092

Amiri, N., Moradi, A., Tabasi, S. A. S., & Movaffagh, J. (2018). Modeling and process optimization of electrospinning of chitosan-collagen nanofiber by response surface methodology. Materials Research Express, 5(4), 045404. DOI: https://doi.org/10.1088/2053-1591/aaba1d

Fatile, B. O., Pugh, M., & Medraj, M. (2021). Optimization of the Electrospun Niobium–Tungsten Oxide Nanofibers Diameter Using Response Surface Methodology. Nanomaterials, 11(7), 1644. DOI: https://doi.org/10.3390/nano11071644

Filip, P., & Peer, P. (2019). Characterization of poly (ethylene oxide) nanofibers—Mutual relations between mean diameter of electrospun nanofibers and solution characteristics. Processes, 7(12), 948. DOI: https://doi.org/10.3390/pr7120948

He, H., Wang, Y., Farkas, B., Nagy, Z. K., & Molnar, K. (2020). Analysis and prediction of the diameter and orientation of AC electrospun nanofibers by response surface methodology. Materials & Design, 194, 108902. DOI: https://doi.org/10.1016/j.matdes.2020.108902

Kalantary, S., Jahani, A., & Jahani, R. (2020). MLR and Ann approaches for prediction of synthetic/natural nanofibers diameter in the environmental and medical applications. Scientific Reports, 10(1), 1-10. DOI: https://doi.org/10.1038/s41598-020-65121-x

Kalantary, S., Jahani, A., Pourbabaki, R., & Beigzadeh, Z. (2019). Application of ANN modeling techniques in the prediction of the diameter of PCL/gelatin nanofibers in environmental and medical studies. RSC advances, 9(43), 24858-24874. DOI: https://doi.org/10.1039/C9RA04927D

Ketabchi, N., Naghibzadeh, M., Adabi, M., Esnaashari, S. S., & Faridi-Majidi, R. (2017). Preparation and optimization of chitosan/polyethylene oxide nanofiber diameter using artificial neural networks. Neural Computing and Applications, 28(11), 3131-3143. DOI: https://doi.org/10.1007/s00521-016-2212-0

Khalili, S., Khorasani, S. N., Saadatkish, N., & Khoshakhlagh, K. (2016). Characterization of gelatin/cellulose acetate nanofibrous scaffolds: Prediction and optimization by response surface methodology and artificial neural networks. Polymer Science Series A, 58(3), 399-408. DOI: https://doi.org/10.1134/S0965545X16030093

Naderi, N., Agend, F., Faridi-Majidi, R., Sharifi-Sanjani, N., & Madani, M. (2008). Prediction of nanofiber diameter and optimization of electrospinning process via response surface methodology. Journal of nanoscience and nanotechnology, 8(5), 2509-2515. DOI: https://doi.org/10.1166/jnn.2008.536

Nasouri, K., Bahrambeygi, H., Rabbi, A., Shoushtari, A. M., & Kaflou, A. (2012). Modeling and optimization of electrospun PAN nanofiber diameter using response surface methodology and artificial neural networks. Journal of Applied Polymer Science, 126(1), 127-135. DOI: https://doi.org/10.1002/app.36726

Sukigara, S., Gandhi, M., Ayutsede, J., Micklus, M., & Ko, F. (2004). Regeneration of Bombyx mori silk by electrospinning. Part 2. Process optimization and empirical modeling using response surface methodology. Polymer, 45(11), 3701-3708. DOI: https://doi.org/10.1016/j.polymer.2004.03.059

Thompson, C. J., Chase, G. G., Yarin, A. L., & Reneker, D. H. (2007). Effects of parameters on nanofiber diameter determined from electrospinning model. Polymer, 48(23), 6913-6922.
DOI: https://doi.org/10.1016/j.polymer.2007.09.017

Zeraati, M., Pourmohamad, R., Baghchi, B., Chauhan, N. P. S., & Sargazi, G. (2021). Optimization and predictive modelling for the diameter of nylon-6, 6 nanofibers via electrospinning for coronavirus face masks. Journal of Saudi Chemical Society, 25(11), 101348. DOI: https://doi.org/10.1016/j.jscs.2021.101348